Controlled Self-assembly of Charged Particles

Nikolay V. Shestopalov, Ph.D.
The University of Texas at Austin, 2010

Supervisors: Gregory J. Rodin
Graeme Henkelman

Self-assembly is a process of non-intrusive transformation of a system from a disordered to an ordered state. For engineering purposes, self-assembly of microscopic objects can benefit significantly from macroscopic guidance and control. This dissertation is concerned with controlling self-assembly in binary monolayers of electrically charged particles that follow basic laws of statistical mechanics.

First, a simple macroscopic model is used to determine an optimal thermal control for self-assembly. The model assumes that a single rate-controlling mechanism is responsible for the formation of spatially ordered structures and that its rate follows an Arrhenius form. The model parameters are obtained using molecular dynamics simulations. The optimal control is derived in an analytical form using classical optimization methods. Two major lessons were learned from that work: (i) isothermal control was almost as effective as optimal time-dependent thermal control, and (ii) neither electrostatic interactions nor thermal control were particularly effective in eliminating voids formed during self-assembly.

Accordingly, at the next stage, the focus is on temperature-pressure control under isothermal-isobaric conditions. In identifying optimal temperature and pressure conditions, several assumptions, that allow one to relate the optimal conditions to the phase diagram, are proposed. Instead of verifying the individual assumptions, the entire approach is verified using molecular dynamics simulations. It is estimated that under optimal isothermal-isobaric conditions the rate of self-assembly is about five time faster than that under optimal temperature control conditions.

It is argued that the proposed approach of relating optimal conditions to the phase diagram is applicable to other systems. Further, the work reveals numerous and useful parallels between self-assembly and crystal physics, which are important to exploit for developing robust engineering self-assembly processes.

Table of Contents

List of Tables

List of Figures

Chapter 1

Introduction

1.1 Self-assembly phenomena

1.1.1 Definition of self-assembly

In general, the term self-assembly refers to a non-intrusive process that transforms a system of multiple components from a less to a more ordered state. By non-intrusive we mean that the process does not require human intervention at the scale of the individual components. In general, structural regularity is attained due to the interactions among the system components. In order to ensure the formation of well-ordered structures the interactions must be reversible, i.e. the components must be able to associate as well as dissociate in the course of self-assembly. This is generally achieved by subjecting the system to external agitation, which, in effect, produces a random force field acting on the components. The strength of this force field must be commensurate with the strength of the interactions. This allows the components to dissociate from poorly ordered structures en route to the desired configuration.

1.1.2 Examples of self-assembly

Self-assembly is ubiquitous in nature and occurs on a wide variety of scales ranging from atomistic to macroscopic. It is representative of many chemical and biological phenomena.

One of the most well-known examples of self-assembly is crystal growth, which occurs naturally or can be engineered [47]. Crystals are formed as a result of self-assembly of atoms or basic molecules, with the binding forces of covalent or ionic nature. These forces are considered strong because the associated binding energy is roughly one hundred times larger than the thermal energy at room temperature. Supramolecular self-assembly differs from crystallization as it uses complex organic macromolecules as building blocks [50]. The binding forces among macromolecules are often of non-covalent nature, form a richer set and are orders of magnitude weaker than those in a crystal. As a result a broad spectrum of diverse structures is attained and structural rearrangements easily occur at room temperature.

For living organisms, it is essential to rapidly adapt to the environment. Therefore, the ease of rearrangements is essential. In addition, many biological systems are organized hierarchically through self-assembly at different scales. In particular, on the microscopic scale, amino acids and nucleotides self-assemble into proteins and nucleic acids, respectively. On the mesoscopic scale, proteins and nucleic acids regulate cell synthesis and signal transduction. On the macroscopic scale, the cells self-assemble into the living organism [11].

Self-assembly can be governed by a variety of interactions among the system components. It has been observed in systems governed by capillary [87], electrostatic [5], magnetic [16], optical [65], gravitational [34], entropic [58], van der Waals [36], hydrophobic [51] and hydrodynamic [82] interactions.

Figure 1.1 shows an example of self-assembly of vesicles, which can be thought of as lamellar bubbles of liquid suspended in another liquid. They are important in living organisms because they can store, transport and digest cellular products and waste. A basic building block of vesicles is an amphiphile molecule which contains a hydrophilic *head* group and a pair of hydrophobic *tail* groups. When the amphiphiles are placed in water they assemble into a *unilamellar* vesicle through a balance of hydrophobic/hydrophilic and surface tension effects. Formation of *multilamellar* vesicles occurs in a hierarchical fashion by addition of concentric amphiphilic shells of increasing radii [66].

Other common self-assembly systems include colloids [33], block copolymers [10] and monolayers [4].

1.1.3 Applications of self-assembly

Modern technology is in constant search of new fabrication methods that are robust at progressively smaller scales. Therefore many current methods become ineffective and even obsolete for manufacturing small components, especially at the nanometer scale. For instance, fabrication based on robotic manipulation of the individual components becomes ineffective because conventional "pick and place" methods are difficult to apply to components less

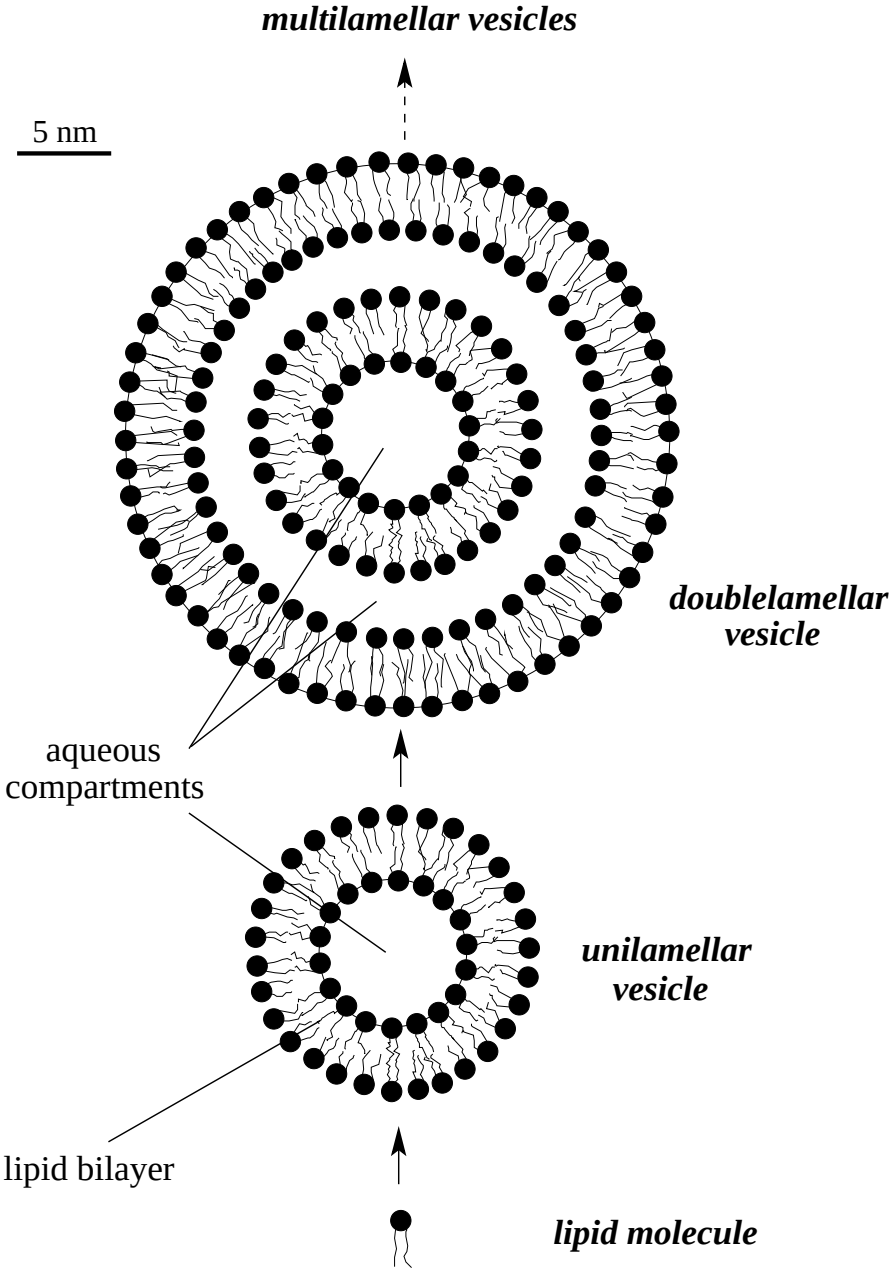

Figure 1.1: Example of self-assembly in nature: formation of vesicles from lipid molecules.

than 100 μm in size. Other existing methods, such as microlithography are also limited in scale due to the problem with light diffraction that arises scales below 10 nanometers.

In contrast, self-assembly presents a number of significant advantages, as it is capable of creating regular structures across multiple scales. Typically, regularity leads to important mechanical, electronic, optical and other properties and functionalities, that are critical to mechanical and micromechanical electrical systems (MEMS) [78]. Figure 1.2 shows an example where self-assembly was used to build a cylindrical light-emitting diode (LED) display [49], by placing 1500 silicon cubes 300 μm in size inside a large cylindrical container. One side of each cube was coated with a metal contact which wetted and bonded to a solder-based receptor on the cylindrical substrate. Bonding was due to surface tension of the solder, which was maintained in a liquid state at 90°C. In order for the components to find their target sites, external agitation in the form periodic tumbling motion was required.

Self-assembly can be of great potential use for photonic band gap materials and devices [24, 48]. The term "band gap" refers to a certain range of wavelengths. Due to lattice periodicity the waves in the range are not transmitted through the material. As such, photonic band gap materials can be used for optical wave guiding [1]. Currently, the use of self-assembly for photonic band gap materials and devices is limited by difficulties in controlling inter-particle spacing and attaining long-range order. Both are essential for optical wave propagation [54]. Perhaps this obstacle can be overcome with

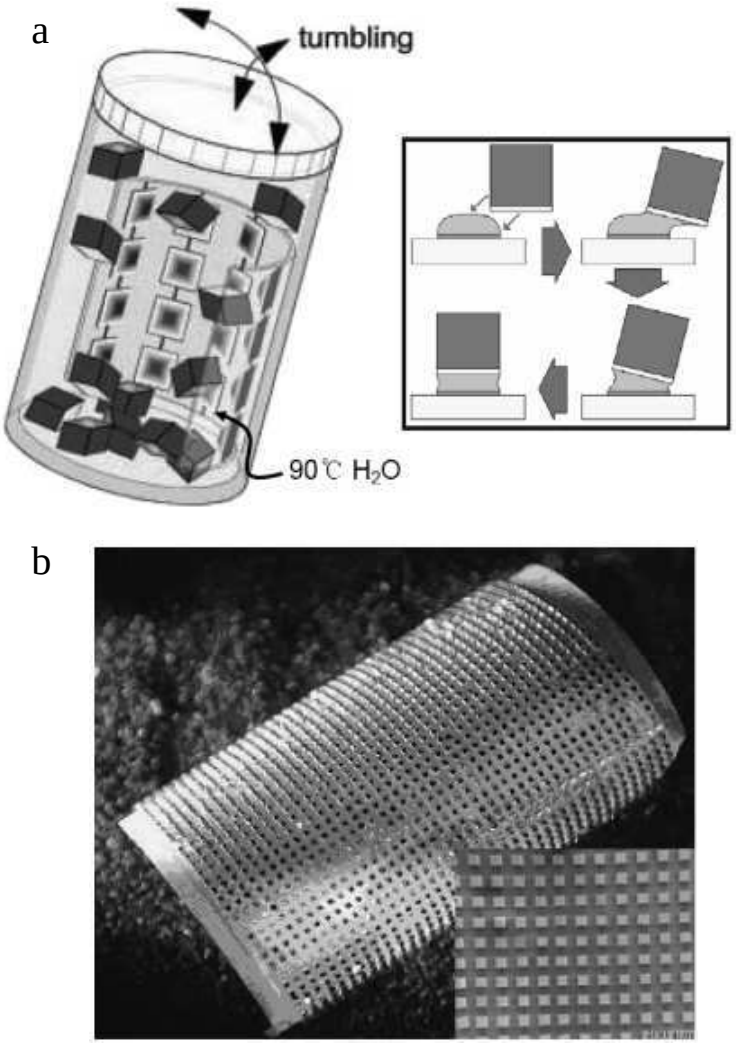

Figure 1.2: Cylindrical LED display built using self-assembly [49]: *a*) Bonding of silicon cubes to the cylinder in the presence of tumbling; *b*) Macroscopic view of the product.

guided or controlled self-assembly processes. On the nanometer scale, self-assembly is crucial for creating nanowires, nanotubes, and coatings [18, 76]. Similarly, better quality products can be achieved with guidance and control of self-assembly.

Observing how nature uses self-assembly has stimulated interest in creating adaptable, self-healing and self-replicating structures [59]. Figure 1.3 shows an example of adaptable self-assembly using a combination of capillary and hydrophilic/hydrophobic effects [17]. The system consists of identically-shaped components made from poly(dimethylsiloxane) (PDMS) doped with alumina. The edges of the components are functionalized into hydrophilic or hydrophobic sets, which are denoted by, respectively, thin and thick lines in the figure. The components are suspended in water and a hydrophobic liquid perfluorodecalin (PFD). As the two liquids are immiscible and the density of alumina-doped PDMS is intermediate to that of water and PFD, the components settle at the interface between the two liquids with their centers of mass slightly below the interface, Fig 1.3 (a). In this configuration the attraction between the hydrophilic edges is stronger than it is between the hydrophilic edges and patterns in Figure 1.3 (d,e,f) result. By adding sodium metatungstate to water it possible to change the density balance so that the components' center of mass lifts above the interface Figure 1.3 (b). In this case, the attraction between the hydrophobic edges is strongest and the patterns change to those in Figure 1.3 (d',e',f').

Finally, a different perspective on self-assembly was introduced through

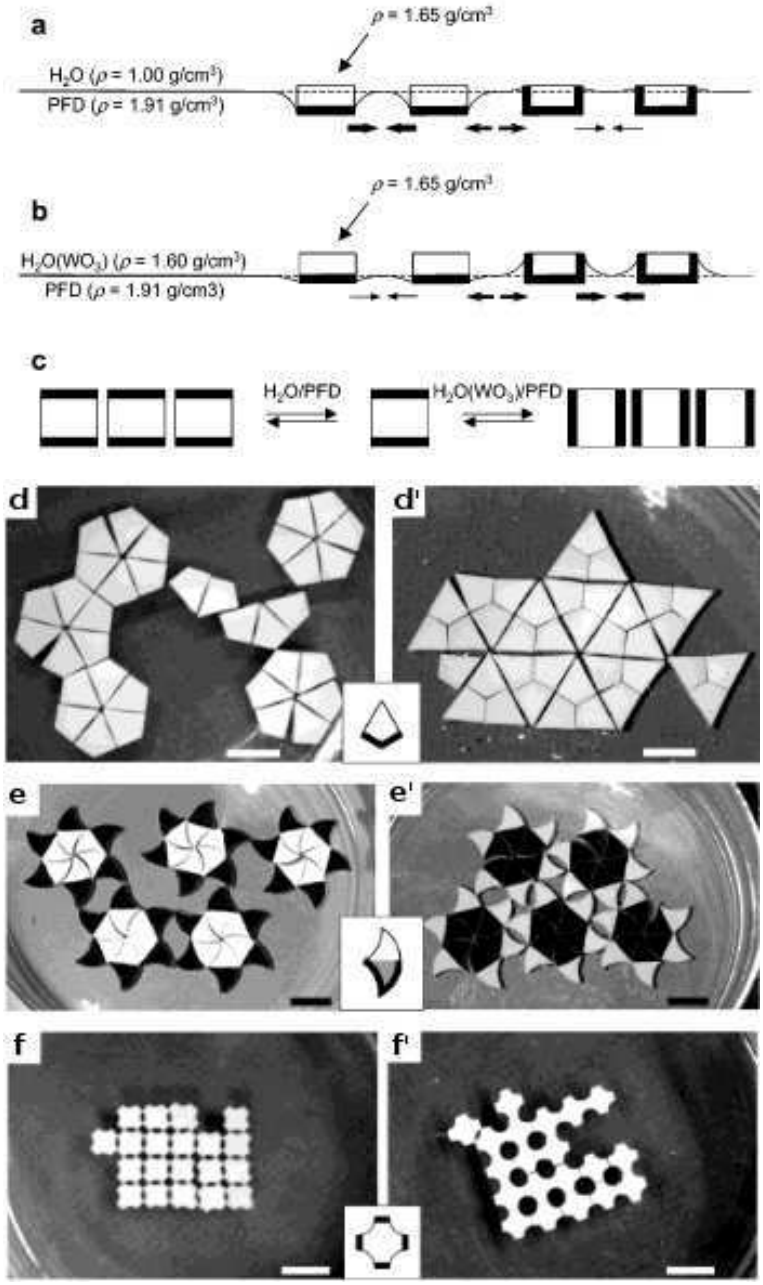

Figure 1.3: Example of adaptable self-assembly using a combination of capillary and hydrophilic/hydrophobic effects at the interface between two immiscible liquids - water and perfluorodecalin (PFD).

its potential to perform computation. In this view, any periodic tiling formed through self-assembly represents a simulation of a Turing machine [75].

1.1.4 Control of self-assembly systems

For many engineered products, especially those that require long-range ordering, self-assembly must be guided and/or controlled. In nature, this is accomplished by a variety of mechanisms including hierarchical assembly, simultaneous action of multiple force fields, geometric constraints, shape complementarity and templating. It is the hope in engineering these mechanisms can be applied to produce optimality and a high degree of ordering.

To achieve a desired ordered state two conditions must be met. First, that state must be stable. This condition is related to equilibrium, or, when under non-equilibrium settings, to spatial or temporal oscillatory patterns [62]. Second, the desired state must be attainable, and preferably in an optimal manner. For example, in the shortest amount of time or with the minimum possible energy. The second condition is of kinetic nature.

One can meet the first condition by controlling the component shapes, compositions, interactions, geometric constraints, including templating. Generally, the desired structure forms when some stationarity condition is met. When in equilibrium, this simply requires the free energy to be of the system to be at minimum. Under non-equilibrium settings (more frequently encountered in nature) the self-assembled structure is dependent upon a flux of external energy through the system. For instance, cellular activity with its superior

spatial and temporal organization is dependent upon a continuous supply of energy in the form of nutrients. If the supply is terminated the activity ceases and the cell disintegrates. Strictly speaking, the consensus on the stationarity condition under non-equilibrium conditions has not yet been reached. It has been proposed that under these conditions, the systems assumes spatial or temporal regularity in order to minimize entropy production [40, 59].

One can meet the second condition by controlling external agitation so that it allows one to escape undesired meta-stable equilibrium states in route to the desired state. Typically, the agitation mechanism does not significantly affect the final state, but rather enhances the kinetics of its formation. In particular, external agitation is responsible for the reversibility of the interactions among the components. Typically external agitation should accelerate the slowest process of self-assembly, but more sophisticated agitation mechanisms may target several processes and operate in a hierarchical manner. For example, self-assembly of particle monolayers may proceed rapidly with forming small ordered clusters, but slowly with their coalescence into a crystalline structure with a long range order. Then the agitation mechanism must target the coalescence stage. Such behavior has been observed in self-assembly of colloidal suspensions [6, 26], block copolymers [8] and protein solutions [3].

1.2 Experiments of Whitesides' et al.

This work was motivated by self-assembly in model systems proposed by Grzybowski *et al* [14]. The purpose of those experiments was to demon-

strate self-assembly at the mesoscale (10^{-6}–10^{-3} m). In those systems, contact electrification was used as the driving force for self-assembly. Millimeter-size spherical particles were placed at the bottom of a large square container. The walls of the container were coated with gold. As the container was agitated mechanically in the horizontal plane, initially uncharged particles acquired electric charge by colliding with the walls of the container. The experimental setup of Grzybowski *et al.* is shown in Figure 1.4.

The particle materials were chosen so that one could control the charge sign and magnitude, and the rate of charging. The charging history for polymethylmethacrylate (PMMA) and Teflon particles are shown in Figure 1.5. For these materials, the PMMA particles were charged positively, while the Teflon particles were charged negatively, and the rates of charging for the two particle types were roughly equal. By using the same number of PMMA and Teflon particles, Grzybowski *et al* were able to lead the self-assembly process to a perfectly ordered square lattice. They observed formation of small ordered clusters of particles after $t \approx 20$ s when the charging process was approaching a plateau. However, to form a well-ordered square lattice, increased agitation was required for several more minutes. Thus agitation was necessary for two reasons. First, is to create the oppositely charged particles. Without this function, one would not be able to realize a stable equilibrium state. Second, it serves the purpose of a random force that guarantees reversibility of the electrostatic interactions on the timescale of the experiment, $\mathcal{O}(100)$ s. Without this function, one would not have a proper kinetics to reach the desired

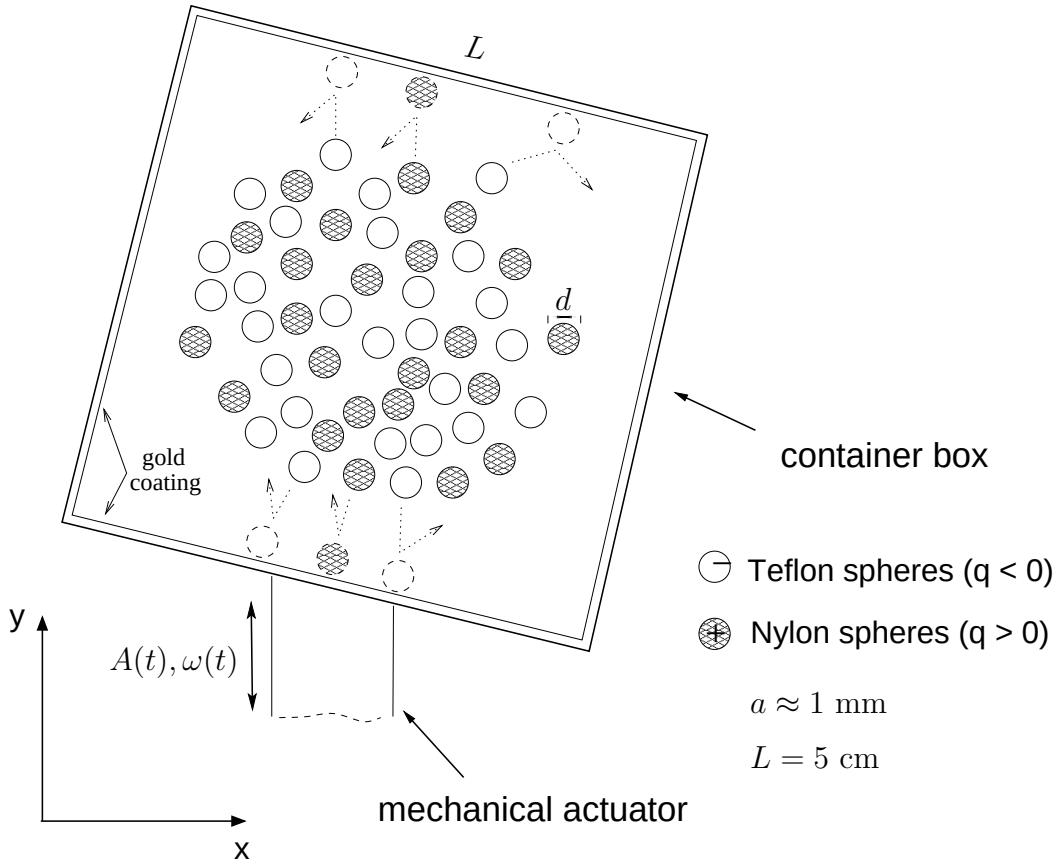

Figure 1.4: Basic self-assembly systems of Grzybowski *et al.*

state.

The charging kinetics in an experiment with 40 Teflon and 80 polypropylene (PP) spheres is shown in Figure 1.6. As the Teflon spheres acquired charge faster than the PP spheres, the ratio of the charges on these two particle types varied in the course of self-assembly. When this ratio was close to 2, the particles assembled into a hexagonal lattice. As agitation continued, the charges on the particles equalized. At this point, the hexagonal lattice disassembled and approximately half of PP spheres were expelled towards the walls of the container. After another several minutes of shaking, a square lattice formed. The process was very sensitive to shaking intensity. When shaking was not sufficiently vigorous, the system was kinetically trapped in a hexagonal lattice which never changed to square even when the magnitude of the charges equalized. If, on the other hand, if the agitation was too vigorous, the charges on the particles quickly reached their steady-state values. In this case, the system never formed a hexagonal lattice but assumed a square lattice directly. This experiment demonstrates the possibility of dynamical switching between the products of self-assembly. It also confirms the notion that the choice of parameters that control kinetics has a significant bearing on the outcome of the self-assembly.

1.3 Model systems

In principle, the macroscopic systems of Grzybowski *et al.* could be modeled using classical mechanics. However, this requires modeling and sim-

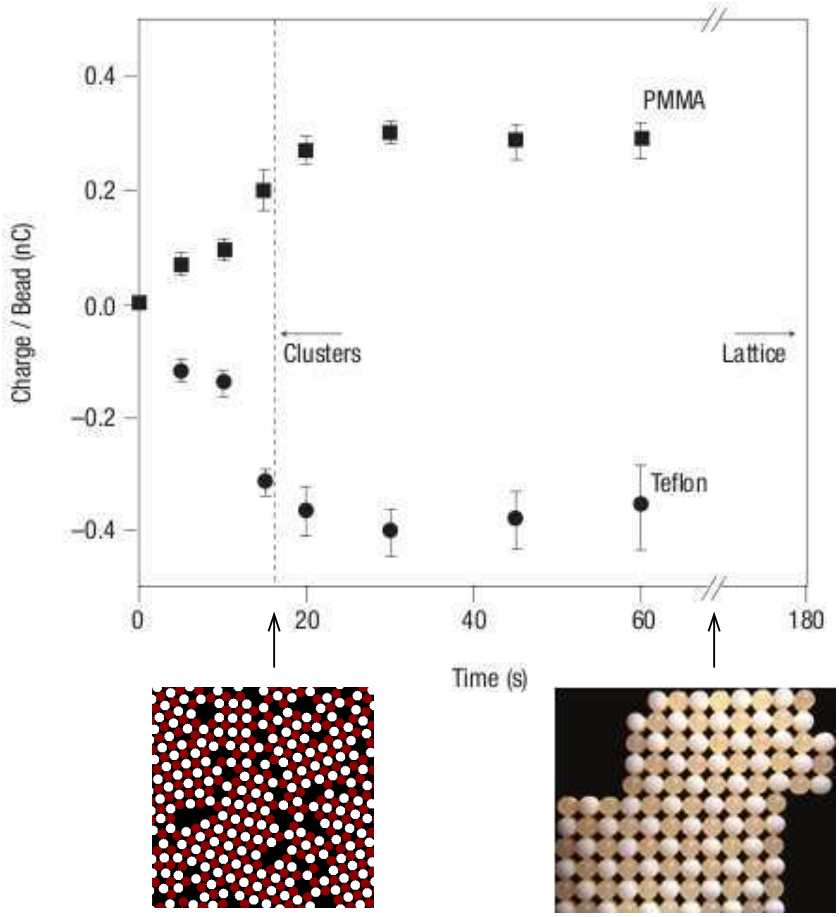

Figure 1.5: Formation of a macroscopic 2-D square Coulombic crystal.

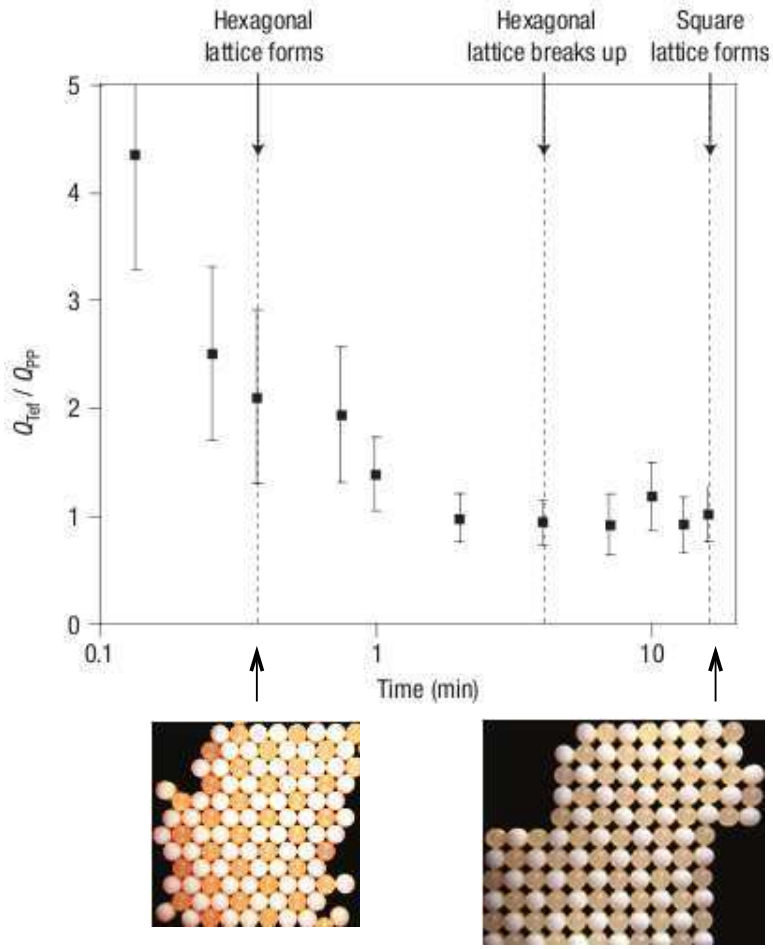

Figure 1.6: Dynamic self-assembly of macroscopic 2-D hexagonal and square Coulombic crystals.

ulation of friction and contact, which is a challenging task, especially for large particle systems. Furthermore, it is not our goal to model the specific systems used by Grzybowski *et al.*, but rather to understand the general principles of controlled self-assembly. In this regard, it is advantageous to consider systems obeying basic laws of thermodynamics and statistical mechanics. Furthermore, such systems are more appealing for applications involving very large numbers of microscopic components (*c.f.* Section 1.1.3). Accordingly, the role of agitation is assumed by thermal rather than mechanical vibrations.

Let us estimate the particle size in systems similar to those of Grzybowski *et al.* for which thermal agitation would be meaningful. Since contact electrification is largely a surface a phenomenon, we expect that the charges on the particles can be expressed as $q = \alpha d^2$, where d is the particle diameter and α is a proportionality constant. In Chapter 2 we will show that ordered lattice states can be obtained when the thermal energy of the system is about 1% of the electrostatic interaction energy between two particles in contact. Based on this relationship, the particle diameter is estimated as

$$d \approx \left(\frac{k_B T \epsilon_0}{2 \times 0.01 \times \alpha^2} \right)^{1/3} \approx 10^{-8}\ m \tag{1.1}$$

This estimate is valid at room temperature and the value of $\alpha \approx 10^{-3}\ Cm^{-2}$ was obtained from the experimental data of Grzybowski *et al.* Therefore, at the nano-scale the role of mechanical agitation used in systems of Grzybowski *et al.* can be safely assumed by thermal vibrations. To this end, let us point to experiments involving self-assembly of binary nanoparticles, in which ordering

was realized in at an elevated temperature $T = 70°C$ without any additional agitation [9].

The instantaneous internal energy U of the system is determined by summing all pairwise interactions. The energy between a pair of particles is the sum of the electrostatic and contact energies:

$$U(r) = U_e(r) + U_c(r) \tag{1.2}$$

The electrostatic energy of two particles with charges q_i and q_j is computed using Coulomb's law,

$$U_e(r) = \frac{q_i q_j}{\epsilon_0 r} \tag{1.3}$$

where ϵ_0 is the vacuum permittivity and r is the distance between the centers of the particles. The contact energy is defined by penalizing the particle overlap:

$$U_c(r) = \kappa \frac{q^2}{\epsilon_0 d} \left(\frac{\delta}{d}\right)^3, \tag{1.4}$$

where $\delta = d - r$ is the penetration distance between two overlapping surfaces. The penalty constant was set $\kappa = 10^3$. This form of interaction is termed "soft repulsion" and is frequently used in Molecular Dynamics simulations of interacting spherical particles [77, 81].

The particles were divided into two groups, A and B. Let n_A (n_B) and q_A (q_B) be, respectively the number and the charge of particles belonging to the group A (B). In this case, the parameters that control the final product of self-assembly are the ratios n_A/n_B and q_A/q_B. We consider two different cases corresponding to the lattices observed in the experiments of Grzybowski *et al.*

i)

$$n_A = n \qquad n_B = n \qquad q_A = q \qquad q_B = -q \tag{1.5}$$

ii)

$$n_A = n \qquad n_B = 2n \qquad q_A = q \qquad q_B = -q/2 \tag{1.6}$$

Here, q is a unit charge. Aside from varying in number and electric charge the particles in the two groups were treated as identical spheres of diameter d and mass m. For large n, a perfectly ordered state corresponding to case i) is a square lattice in which each particle of type A is in contact with four particles of type B, and vice versa. A perfectly ordered state for case ii) is a hexagonal lattice in which each particle of type A is in contact with six particles of type B, and each particle of type B is in contact with three particles of type A and three particles of type B.

We use the particle diameter d as a unit of length, the particle mass m as a unit of mass, and the time $q^{-1}\sqrt{\epsilon_0 m d^3}$ as a unit of time. The temperature T is measured in the corresponding units of energy.

1.4 Background

In this section we lay the methodological basement for the entire dissertation.

1.4.1 Theoretical background

It is possible to define the pressure and the temperature of the system both from the macroscopic and the microscopic points of view.

1.4.1.1 Classical thermodynamics

From the point of view of classical thermodynamics, the following macroscopic relations apply [22]:

$$P = -\left(\frac{\partial U}{\partial V}\right)_S \tag{1.7}$$

$$T = -\left(\frac{\partial U}{\partial S}\right)_V , \tag{1.8}$$

where P is pressure, T is temperature, U is internal energy, V is volume and S is entropy. Thermodynamic identity states that

$$\mathrm{d}U = \mathrm{d}Q + \mathrm{d}W = T\mathrm{d}S - P\mathrm{d}V\,. \tag{1.9}$$

In cases where the volume is not held constant it is convenient to use the heat function, or enthalpy

$$Q = U + PV \equiv H\,, \tag{1.10}$$

and

$$\mathrm{d}H = \mathrm{d}U + P\mathrm{d}V + V\mathrm{d}P = T\mathrm{d}S + V\mathrm{d}P\,. \tag{1.11}$$

If the process occurs at constant pressure, $\mathrm{d}H = T\mathrm{d}S$.

When T and P are the free variables the appropriate thermodynamic potential is the *Gibbs free energy*:

$$G = H - TS\,, \tag{1.12}$$

and

$$\mathrm{d}G = \mathrm{d}H - S\mathrm{d}T - T\mathrm{d}S = -S\mathrm{d}T + V\mathrm{d}P\,. \tag{1.13}$$

1.4.1.2 Coexistence of phases and Clausius-Clapeyron equation

Consider a point on the coexistence curve between two phases. The condition for equilibrium is

$$\mu_1(P,T) = \mu_2(P,T)\,, \tag{1.14}$$

where μ_1 and μ_2 are the chemical potentials. Differentiating both sides with respect to the temperature (on the coexistence curve pressure is not an independent variable but a function of the temperature):

$$\frac{\partial \mu_1}{\partial T} + \frac{\partial \mu_1}{\partial P}\frac{\mathrm{d}P}{\mathrm{d}T} = \frac{\partial \mu_2}{\partial T} + \frac{\partial \mu_2}{\partial P}\frac{\mathrm{d}P}{\mathrm{d}T} \tag{1.15}$$

Making use of 1.13:

$$-S_1 + V_1\frac{\mathrm{d}P}{\mathrm{d}T} = -S_2 + V_2\frac{\mathrm{d}P}{\mathrm{d}T}\,, \tag{1.16}$$

or

$$\frac{\mathrm{d}P}{\mathrm{d}T} = \frac{S_1 - S_2}{V_1 - V_2} \tag{1.17}$$

The latent heat of the transition from one phase to the other is $\Delta H = (S_1 - S_2)\,T$. Hence we obtain what is known as the *Clausius-Clapeyron equation*:

$$\frac{\mathrm{d}P}{\mathrm{d}T} = \frac{\Delta H}{T(V_1 - V_2)}. \tag{1.18}$$

We remark on the case of equilibrium of a solid, 1, with its vapor, 2. Normally, $V_1 \ll V_2$. If, in addition, the behavior of the vapor can be

approximated by that of an ideal gas, (1.18) becomes:

$$\frac{\mathrm{d}P}{\mathrm{d}T} = \Delta H \frac{P}{k_B T^2}\,, \tag{1.19}$$

or

$$\frac{\mathrm{d}\log P}{\mathrm{d}T} = \frac{\Delta H}{k_B T^2}\,. \tag{1.20}$$

Hence, in a temperature interval over which the latent heat may be considered constant, the functional form of the coexistence curve is exponential ($P \sim \exp\left[-\Delta H/k_B T\right]$).

1.4.2 Statistical Thermodynamics

For a $D-$dimensional system consisting of N particles occupying volume V, the temperature and the pressure can be obtained by averaging [20]:

$$T = \sum_{i=1}^{N} \frac{m_i v_i^2}{k_B N_f} = \frac{\langle 2K \rangle}{k_B N_f}\,, \tag{1.21}$$

$$P = \frac{N k_B T}{V} + \frac{1}{DV} \left\langle \sum_{i<j} \boldsymbol{f}(\boldsymbol{r}_{ij}) \cdot \boldsymbol{r}_{ij} \right\rangle . \tag{1.22}$$

Here m_i and v_i are, respectively, the mass and velocity of particle i, $\boldsymbol{f}(\boldsymbol{r}_{ij})$ is the force between particles i and j at a distance $\boldsymbol{r}_{ij}$ and N_f is the number of degrees of freedom per particle.

The following relations hold with respect to the fluctuations in enthalpy and volume under isothermal-isobaric conditions [68]:

$$\langle \delta H^2 \rangle = k_B T^2 C_p\,, \tag{1.23}$$

$$\langle \delta V^2 \rangle = k_B T V \beta_T\,, \tag{1.24}$$

where C_p is the isobaric heat capacity, β_T is the isothermal compressibility. Both (1.23) and (1.24) are expected to diverge as the system approaches a phase transition [39, 57].

1.4.3 Computational methods

1.4.3.1 Molecular Dynamics

Molecular Dynamics is a simulation technique for analyzing many-body systems following the laws of statistical mechanics. In this Section we will outline a procedure of casting these laws as a generalization of classical mechanics.

The classical Lagrangian is defined as

$$\mathcal{L} = K(\dot{q}) - U(q) \tag{1.25}$$

where q is a set of generalized coordinates. The generalized momentum p associated with the generalized coordinates q is

$$p = \frac{\partial \mathcal{L}(q, \dot{q})}{\partial \dot{q}}, \tag{1.26}$$

and the corresponding equation of motion is

$$\dot{p} = \frac{\partial \mathcal{L}(q, \dot{q})}{\partial q} \tag{1.27}$$

The Hamiltonian of a classical mechanical system is defined as

$$\mathcal{H}(q, p) = \frac{1}{2m} p^2 + U(q) \ , \tag{1.28}$$

The Hamiltonian equations of motion are given by first-order differential equations for q and p:

$$\dot{q} = \frac{\partial \mathcal{H}}{\partial p} \tag{1.29}$$

$$\dot{p} = -\frac{\partial \mathcal{H}}{\partial q} \tag{1.30}$$

There are numerous techniques for integrating (1.29)-(1.30) numerically to yield particle trajectories [67]. Reliable integration schemes do not introduce any significant drift into the conserved quantity (1.28) in the course of the simulation. A common scheme for integrating equations of motion is due to Verlet [56].

Self-assembly, however, occurs under slightly different settings. Let us return to the experiments Grzybowski *et al.* The energy of the system is dissipated during collisions between the particles and friction between the particles and the container. If the container is not agitated and the system is left to its own devices, the Hamiltonian is a monotonically decreasing function of time. However, the container is agitated so that there is a continuous influx of kinetic energy into the system. These conditions resemble those of a system in equilibrium with a thermal bath. In such a case, the conserved quantity is not the total Hamiltonian of the system $\mathcal{H}$, but rather the kinetic energy. Of course, the conservation of kinetic energy is not strictly enforced, but it holds "on average". If the particles in the monolayer are modeled as having only two degrees of freedom, the average kinetic energy per particle is

$\langle K \rangle = T$ (equation 1.21). This implies that the process occurs under constant temperature.

To simulate a classical mechanical system under isothermal conditions, one can adopt either a stochastic or a deterministic formulation. Stochastic formulations are based on an assumption that the system interacts with the thermal bath through periodic collisions [35]. Due to the collisions, the velocities of the particles are periodically rescaled towards (or drawn from a Maxwell velocity distribution corresponding to) a given temperature T. The frequency of the collisions is a characteristic of the strength of the coupling between the system and the thermal bath.

Deterministic formulations are based on the use of an extended Lagrangian. We are going to briefly describe the original approach of Nose [80]. An extended Lagrangian is defined as:

$$\mathcal{L} = Ks^2 - U + \frac{1}{2}Q\dot{s}^2 - (N+1)k_BT\ln s \tag{1.31}$$

In this equation, s is an additional coordinate that couples the particle kinetic energy to the heat bath, and Q is an effective "mass" associated with s.

The Hamiltonian of the extended system is

$$\mathcal{H} = \sum_{i=1}^{N} \frac{p_i^2}{2m_i s^2} + U + \frac{p_s^2}{2Q} + (N+1)k_BT\ln s \tag{1.32}$$

By introducing the variables $p_i' = p_i/s$, $p_s' = p_s/s$, $t' = t/s$ and $\xi = sp_s'/Q$, this Hamiltonian takes the form

$$\mathcal{H} = \sum_{i=1}^{N} \frac{p_i'^2}{2m_i} + U + \frac{1}{2}Q\xi^2 + Nk_BT\ln s \tag{1.33}$$

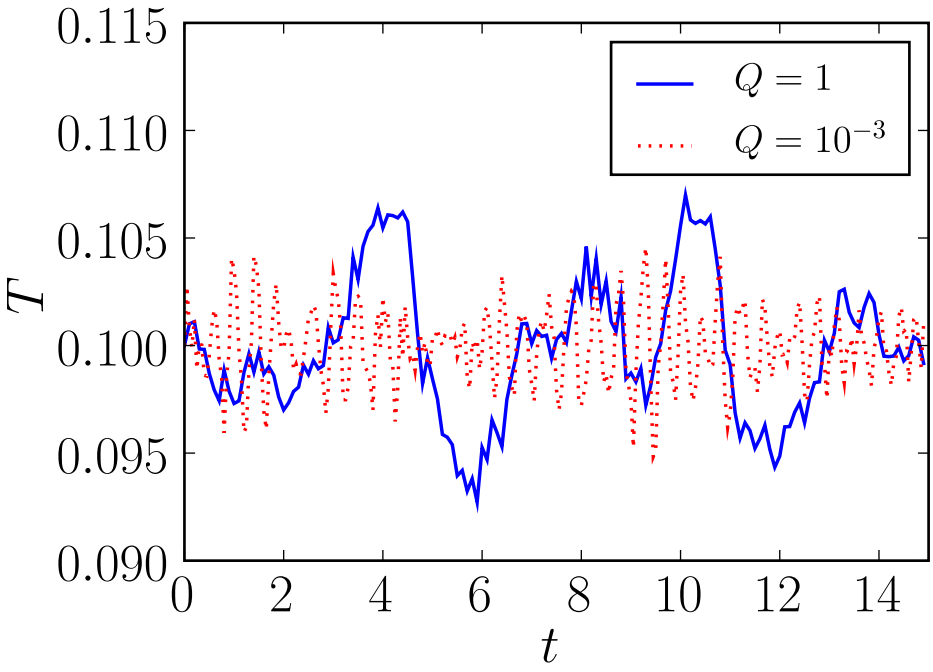

Figure 1.7: The behavior of Nose-Hoover thermostat for two different values of effective "mass" Q.

We note that under isothermal conditions the extended Hamiltonian is a conserved quantity.

The effective mass Q determines how strongly the system is coupled to the heat bath. If the system is visualized as if connected to the heat bath by a Hookean spring, Q is related to the frequency of vibration of the spring ω_s via $Q = T\omega_s^{-2}$. Therefore, for a given temperature smaller Q produce stronger couplings. Figure 1.7 illustrates the difference between two different values of Q in a system of 1250 particles maintained at $T = 0.1$ for 15 time units.

It can be shown that the extended Lagrangian formulation of Nose gen-

erates trajectories that are consistent with the canonical ensemble in statistical mechanics [20].

This formulation is sufficient for implementing thermal control. However, we will show that efficiency of self-assembly may be significantly affected by other macroscopic control parameters. One particular parameter that we are going to study is external pressure. In this case it is possible to further augment the extended Lagrangian formulation (1.31) as in [31]. The trajectories generated from this formulation are consistent with the distribution in the isothermal-isobaric statistical ensemble [20].

1.4.3.2 Sampling enhancement methods

The method of Molecular Dynamics described in the previous section can be used to sample both equilibrium and non-equilibrium properties of the system. The former can be sampled only after the simulation has proceeded long enough so that it can be considered "equilibrated". Other sampling methods may be preferable in cases where only equilibrium properties of the system are of interest and capturing actual dynamics of the system is not essential.

One such equilibrium sampling method is the Metropolis sampling [70]. This method is based on the idea that in equilibrium a random sampling of the phase space is highly inefficient as the vast majority of microstates have very low statistical weights. At each step in the algorithm a set of new coordinates $\boldsymbol{r}_j$ is generated from the existing set $\boldsymbol{r}_i$ according to some probability density function $G(\boldsymbol{r}_i \rightarrow \boldsymbol{r}_j)$. The new configuration is then accepted according to a

probability density function $A(\boldsymbol{r}_i \rightarrow \boldsymbol{r}_j)$. The choice of the probability density functions G and A is not unique but is governed by the condition of detailed balance [20, 52]. In their original work Metropolis *et al.* chose $\boldsymbol{r}_j$ uniformly distributed within a given distance Δ away from $\boldsymbol{r}_i$ and accepted the new configuration with the probability

$$A(\boldsymbol{r}_i \rightarrow \boldsymbol{r}_j) = \min\{1, \exp\left[-\beta(U(\boldsymbol{r}_j) - U(\boldsymbol{r}_i))\right]\} , \tag{1.34}$$

where U is the potential energy of the system and $\beta = (k_B T)^{-1}$ is the inverse temperature.

The acceptance probability consistent with the isothermal-isobaric statistical ensemble is

$$A(\boldsymbol{r}_i \rightarrow \boldsymbol{r}_j) = \min\{1, \left[\frac{V(\boldsymbol{r}_j)}{V(\boldsymbol{r}_i)}\right]^N \exp\left[-\beta(H(\boldsymbol{r}_j) - H(\boldsymbol{r}_i))\right]\} , \tag{1.35}$$

where $H(\boldsymbol{r}_i)$,$V(\boldsymbol{r}_i)$ and $H(\boldsymbol{r}_j), V(\boldsymbol{r}_j)$ are the enthalpies and volumes corresponding, respectively, to configurations i and j [20].

At low temperatures Metropolis algorithm can have prohibitively low equilibration times. Replica Exchange Molecular Dynamics (*REMD*) is a sampling technique designed to overcome this problem [2, 23, 52]. It is based on the observation is that at lower temperatures the system is unable to overcome large energy barriers. In *REMD* several replicas of the system are simulated concurrently at a range of temperatures. Efficient sampling at higher temperatures can be propagated to lower temperatures by periodically exchanging the configurations among the replicas. Consider replicas i and j simulated,

respectively, at inverse temperatures β_i and β_j. The following choice of the probability for accepting a swap of configurations between replicas i and j satisfies the condition of detailed balance:

$$A(\boldsymbol{r}_i \leftrightarrow \boldsymbol{r}_j) = \min\{1, \exp\left[-(\beta_i - \beta_j)(U(\boldsymbol{r}_i) - U(\boldsymbol{r}_j))\right]\} \tag{1.36}$$

The acceptance probability consistent with the isothermal-isobaric statistical ensemble is

$$A(\boldsymbol{r}_i \leftrightarrow \boldsymbol{r}_j) = \min\{1, \exp\left[-(\beta_i - \beta_j)(H(\boldsymbol{r}_i) - H(\boldsymbol{r}_j))\right]\} \ . \tag{1.37}$$

1.5 Overview of the dissertation

The overall theme of this dissertation is control of self-assembly in model systems similar to those used by Grzybowski *et al.* In Chapter 2 we develop an optimal control strategy based on thermal control alone. This strategy is based on a macroscopic model, which is calibrated using Molecular Dynamics, and an optimal schedule is derived using classical optimization methods. The performance of the derived schedule is evaluated and directions of principal improvements are identified. In Chapter 3 we consider isothermal-isobaric control. A model is developed to rationalize significant improvements over pure thermal control. In Chapter 4 we summarize key results of our work and outline possible directions for future work.